

Central noradrenaline transporter availability in highly obese, non-depressed individuals

Swen Hesse^{1,2} · Georg-Alexander Becker¹ · Michael Rullmann^{1,2,3} · Anke Bresch¹ · Julia Luthardt¹ · Mohammed K. Hankir² · Franziska Zientek² · Georg Reißig² · Marianne Patt¹ · Katrin Arelin^{3,4} · Donald Lobsien⁵ · Ulrich Müller⁶ · S. Baldofski^{2,8} · Philipp M. Meyer¹ · Matthias Blüher⁷ · Mathias Fasshauer^{2,7} · Wiebke K. Fenske² · Michael Stumvoll^{2,7} · Anja Hilbert^{2,8} · Yu-Shin Ding⁹ · Osama Sabri^{1,2}

Received: 14 July 2016 / Accepted: 28 November 2016 / Published online: 9 January 2017
© Springer-Verlag Berlin Heidelberg 2017

Abstract

Purpose The brain noradrenaline (NA) system plays an important role in the central nervous control of energy balance and is thus implicated in the pathogenesis of obesity. The specific processes modulated by this neurotransmitter which lead to obesity and overeating are still a matter of debate.

Methods We tested the hypothesis that in vivo NA transporter (NAT) availability is changed in obesity by using positron emission tomography (PET) and S,S-[¹¹C]O-methylreboxetine (MRB) in twenty subjects comprising ten highly obese (body mass index BMI > 35 kg/m²),

metabolically healthy, non-depressed individuals and ten non-obese (BMI < 30 kg/m²) healthy controls.

Results Overall, we found no significant differences in binding potential (BP_{ND}) values between obese and non-obese individuals in the investigated brain regions, including the NAT-rich thalamus (0.40 ± 0.14 vs. 0.41 ± 0.18; *p* = 0.84) though additional discriminant analysis correctly identified individual group affiliation based on regional BP_{ND} in all but one (control) case. Furthermore, inter-regional correlation analyses indicated different BP_{ND} patterns between both groups but this did not survive testing for multiple comparisons.

Conclusions Our data do not find an overall involvement of NAT changes in human obesity. However, preliminary secondary findings of distinct regional and associative patterns warrant further investigation.

✉ Swen Hesse
swen.hesse@medizin.uni-leipzig.de

¹ Department of Nuclear Medicine, University of Leipzig, Liebigstraße 18, 04103 Leipzig, Germany

² Integrated Treatment and Research Centre (IFB) Adiposity Diseases, Leipzig University Medical Centre, Leipzig, Germany

³ Max Planck Institute for Human Cognitive and Brain Sciences, Leipzig, Germany

⁴ Day Clinic for Cognitive Neurology, University of Leipzig, Leipzig, Germany

⁵ Department of Neuroradiology, University of Leipzig, Leipzig, Germany

⁶ Department of Psychiatry and Behavioural and Clinical Neuroscience Institute, University of Cambridge, Cambridge, UK

⁷ Department of Internal Medicine, University of Leipzig, Leipzig, Germany

⁸ Department of Medical Psychology and Medical Sociology, University of Leipzig, Leipzig, Germany

⁹ Departments of Radiology and Psychiatry, New York University School of Medicine, New York, NY, USA

Keywords Noradrenaline · Noradrenaline transporter · PET · PET imaging · Obesity

Introduction

Obesity has reached epidemic proportions yet no sustainable non-surgical treatment is available. The mechanisms of weight gain, in particular the biological underpinnings that lead to overeating, are only partially understood. As potential targets, the central biogenic amines have long been studied for their effects on feeding behaviour, energy balance, and maintenance of body weight [1]. The appetite-suppressing drugs amphetamine, methamphetamine and phentermine all possess a monoaminergic mechanism of action; in particular they potentially cause release of noradrenaline (NA) from synaptic vesicles as well inhibiting/reversing extracellular NA reuptake by

the NA transporter (NAT) at the synaptic cleft [2]. Evidence for a direct involvement of NA in mediating food intake derives mainly from pharmacological and lesioning studies performed in animals. It has been shown in rats that NA acting in the hypothalamic arcuate, ventromedial and paraventricular nuclei stimulates feeding [3–5], whereas it inhibits feeding in the lateral hypothalamic area [3] through α - and β -receptors. Furthermore, ablating hindbrain noradrenergic neurons which project to the hypothalamic arcuate and paraventricular nuclei eliminates orexigenic [5] and potentiates anorexigenic [6] actions of feeding hormones in rats, respectively. Also, electrically silencing NA neurons of the locus coeruleus (LC) reduces brown adipose tissue thermogenesis leading to obesity in mice through reduced energy expenditure [7]. Critically, the NA system is a key substrate that mediates stress and emotional eating downstream of the hypothalamic–pituitary–adrenal (HPA) axis [8]. Thus, it can be speculated that gradual changes in NA tone influences eating behaviour and metabolism which may lead to obesity, but this has yet to be formally investigated in vivo in humans.

Reuptake via the high-affinity NAT is the primary mechanism by which noradrenergic synaptic transmission is terminated. Due to the lack of suitable radiotracers, only one neuroimaging study has investigated the role of the NAT in obese humans so far. Using NAT-specific (S,S)-[¹¹C]O-methylreboxetine ([¹¹C]MRB) and positron emission tomography (PET), first findings in individuals with obesity suggested that NAT is reduced in the thalamus and pulvinar [9]. However, these results have not been replicated thus far in class II to III obesity (BMI >35 kg/m² and BMI >40 kg/m², respectively). Replication is of particular interest since depression, although excluded in the study by a structured clinical interview for DSM-IV Axis-I psychiatric disorder [9], may occur on a sub-threshold level and this potentially interferes with NAT [10].

Our study, therefore, aimed to investigate in an independent, highly selective cohort of non-depressed, metabolically healthy individuals whether those who are heavily obese (BMI >35 kg/m²) or non-obese (BMI <30 kg/m²) differ in NAT availability as measured with [¹¹C]MRB and PET. In order to extend data analysis beyond simple *t* statistics and to analyse the PET data matrix as a whole, we additionally applied discriminant analysis as well as correlative analysis of NAT availability between different brain regions. The Beck Depression Inventory (BDI) was used as a psychometric test for screening of depression beyond clinical manifestation [11].

Materials and methods

This study was performed in accordance with the ICH Guideline for Good Clinical Practice (GCP) and the declaration of Helsinki, approved by the local ethics committee (IFB

PET K7-7, EC number 206-10-08032010) and the German Bundesamt für Strahlenschutz/Federal Office for Radiation Protection (number Z5-22461-2-2011-002). The study was registered at the European clinical trial database (EudraCT 2012-000568-32) and the German Clinical Trials Register (DRKS).

Participants

Twenty participants aged over 18 years were included. Exclusion criteria were current or past neurological or psychiatric illness, i.e. depression (as assessed by a psychiatrist at the first visit), head trauma or vascular encephalopathy, hypertension, diabetes or other medical conditions that may alter brain function, the use of anorectic medication or other interventions for weight loss, centrally acting medication, over-the-counter medication or nutrition supplements over the last 8 weeks, past or present history of alcohol misuse and/or illicit drug abuse, pregnancy and breast-feeding. Study participants were free of any medication or illicit drugs and did not fulfil criteria for binge eating disorder as assessed by structured expert interview (Eating Disorder Examination; EDE) [12]. The amount of alcohol and/or nicotine consumption was recorded for both cohorts.

Structural magnetic resonance imaging (MRI) was acquired using a 3-Tesla (T) Siemens scanner and a T1-weighted three-dimensional (3D) magnetization-prepared rapid gradient echo (MP-RAGE) sequence (time of repetition 2300 ms, time of echo 2.98 ms, 176 slices, field of view 256 × 240 mm, voxel size 1 × 1 × 1 mm) for PET-MRI coregistration and for exclusion of brain pathologies such as diffuse or confluent white matter hyperintensities in T2-weighted images, tumours, and stroke, but not malformation without functional impairment. All study participants were able to understand the protocol and gave written informed consent.

After obtaining informed consent, screening for inclusion/exclusion criteria, physical examination and MRI as described above, eligible study participants underwent PET with [¹¹C]MRB. On the PET scanning day, they were encouraged to have a light breakfast. Prior to scanning, all participants received a general physical examination, including objective weight and height measures for BMI calculation, and fulfilled the BDI close to the PET imaging session.

PET imaging

Both the MRB standard and precursor were prepared following previously described methods [13]; and [¹¹C]MRB was synthesized from [¹¹C]methyl iodide ([¹¹C]CH₃I) by using the TRACERLab FXC automated synthesis module (GE Healthcare, USA). [¹¹C]methyl iodide ([¹¹C]CH₃I) was produced from [¹¹C]CO₂. The final formulated product was

98% radiochemically pure and the average injected mass was $0.027 \pm 0.023 \mu\text{g/kg}$ (Table 1). Dynamic PET was performed after intravenous bolus injection (90 s) of $359 \pm 11 \text{ MBq } [^{11}\text{C}]\text{MRB}$ using the ECAT EXACT HR+ scanner in 3D acquisition mode [Siemens, Erlangen, Germany; intrinsic resolution at the centre 4.3 mm (full-width at half maximum, FWHM), axial resolution: 5–6 mm, field of view: 15.5 cm]. Emission scan duration was 120 min acquiring 26 frames (4×0.25 , 4×1 , 5×2 , 5×5 , 8×10 min). We used a 10-min-transmission scan (from three ^{68}Ga sources), which was performed prior to the emission scan, for attenuation correction and iterative reconstruction (10 iterations, 16 subsets) in a transverse image series (63 slices, 128×128 matrix, voxel size $2.6 \times 2.6 \times 2.4 \text{ mm}^3$) with a Hann filter (cut-off 4.9 mm) for post-processing.

Imaging data processing and analysis

PET and MRI data processing were performed as recently described [14]. In short, individual MRI data sets of the subjects were spatially reoriented (according to the anterior commissure–posterior commissure line) onto a standard brain data set similar to the Talairach space using the image processing software PMOD version 3.3 (PMOD Technologies, Zurich, Switzerland). Hereafter, volumes of interest (VOIs) were drawn manually on consecutive transversal slices of the reoriented individual MRI data sets. PET data were corrected for head motion artifacts using SPM software (Statistical Parametric Mapping; Wellcome Trust Centre for Neuroimaging, London, UK) and then co-registered with the individual MRI data, respective of the related VOI set, to obtain via PMOD the corresponding tissue time activity curves (TACs) from the dynamic PET data. The atlas-driven registration of individual MR images was manually adjusted to account for possible anatomical variability within or between the groups as suggested by morphometric studies in obese vs. non-obese healthy control samples [15]. Kinetic modelling of these regional brain TACs was performed using the multilinear reference tissue model MRTM2 (two parameters) with the occipital cortex and the caudate as reference regions [16–18]. MRTM2 can be derived from the two-tissue compartment model (2TCM) of a target region with rate constants K_1, k_2, k_3, k_4 and the one-tissue compartment model (1TCM) of the reference region (rate constants K'_1, k'_2) if the non-displaceable distribution volume (DV) in both regions is assumed to be equal. The calculated binding potential BP_{ND} depends linearly on the regional NAT availability and is connected to the DV ratio (DVR) of the target and reference region by $\text{BP}_{\text{ND}} = \text{DVR} - 1$ [19, 20]. If not stated otherwise results presented are computed with the occipital cortex as reference (Fig. 1). Head movements of patients and controls increased at the end of the scan (120 min); therefore, we only used TACs up to 90 min (frames 4 to 23) for multi-linear

regression analysis. Additionally, voxel-based correlation analyses in SPM8 was then performed using BP_{ND} maps with age, sex, and smoking status as covariates. Analyses were performed with $p < 0.005$ and $p < 0.001$, uncorrected and with a minimum cluster size of 30 voxels.

Statistical analysis

All data were tested for normal distribution using the Shapiro–Wilk test and the Levene test for homogeneity of variance. A *t* test was used for group comparison between the PET measures of each VOI. To control for confounding effects of age and BDI while comparing groups, an ANCOVA was applied. All these analyses were performed using PASW/SPSS 20 (IBM Corp., Armonk, NY, US).

As secondary analysis to identify whether the NAT status differs in both groups, linear discriminant analysis (LDA) and inter-regional correlative analysis of the BP_{ND} of each VOI were applied. LDA was performed with group membership as a dependent variable. Four discriminant models were employed. First, BP_{ND} values of all brain regions, age and sex were used as independent variables in a stepwise inclusion procedure based on the results of the Shapiro–Wilk test to identify the relevant variables, i.e. brain regions ($F \geq 3.84$ for inclusion, $F \leq 2.71$ for exclusion). Second, based on the results of the forward selection process, three additional discriminant models with the BP_{ND} values of only three or two brain regions as variables were constructed and characterized by their reclassification performance using cross-validation (leave-one-out technique). The quality of a discriminant model was further characterized by Wilk's lambda, the ratio of the sum of squares within and between groups. Wilk's Lambda ranges between 0 and 1, where lower values point out to a better discrimination between the groups. The inter-regional correlation analysis of VOI data separated for both groups was performed using Pearson's correlation coefficient.

Results

Characteristics of the study participants are summarized in Table 1. All subjects completed both PET and MRI scans, but one obese participant was removed from the MR scan shortly before completion of the acquisition.

Overall, neither voxel- or atlas-derived VOI-based comparisons revealed significant BP_{ND} differences between the groups (Table 2). The data distribution between the groups and within each group for distinct NAT-rich brain regions is shown in Fig. 2. Correlative analyses revealed a significant association between BP_{ND} and BDI in the nucleus accumbens (Table 3), which did not survive testing for multiple comparisons. There were no other significant correlations. An ANCOVA correcting for age and BDI did not reveal any

Table 1 Subject characteristics

	Obese individuals ($>35 \text{ kg/m}^2$)	Non-obese individuals ($<30 \text{ kg/m}^2$)	<i>p</i> value ^a
Number of subjects	10	10	
Sex (male/female)	6/4	6/4	1.00 ^b
Age (years)	34.4 (9.0; 22–50)	33.3 (10.0; 21–50)	0.80
Body mass index (kg/m^2)	42.4 (3.7; 35.7–47.8)	23.9 (2.5; 21.7–28.7)	<0.001
Ethnicity		Caucasian	
Smoking habits (zero/low/moderate/strong)	7 / 1 / 0 / 2	5 / 1 / 0 / 4	0.8 ^c
Alcohol consumption (drinks per week)	1 (0–3.4)	3.5 (1.1–10.1)	0.14 ^d
Beck Depression Inventory	10.5 (10.7; 0–32)	5 (6.7; 0–22)	0.20
Activity applied (MBq)	356.7 (14.2)	361.2 (6.6)	0.38
Injected mass ($\mu\text{g/kg}$)	0.03 (0.03)	0.02 (0.02)	0.50

^a *t* test, except ^b Chi-square test, ^c Fisher's test, ^d Mann–Whitney *U* test. Values denote numbers or means (standard deviation; range). Bold values indicate statistical significance ($p < 0.05$)

changes in group comparisons (Table 3). Correlative analyses of inter-regional BP_{ND} distribution revealed more significant associations ($n = 52$ uncorrected and $n = 23$ Bonferroni-corrected) in obese individuals compared with non-obese controls ($n = 27$ and $n = 15$; Fig. 3).

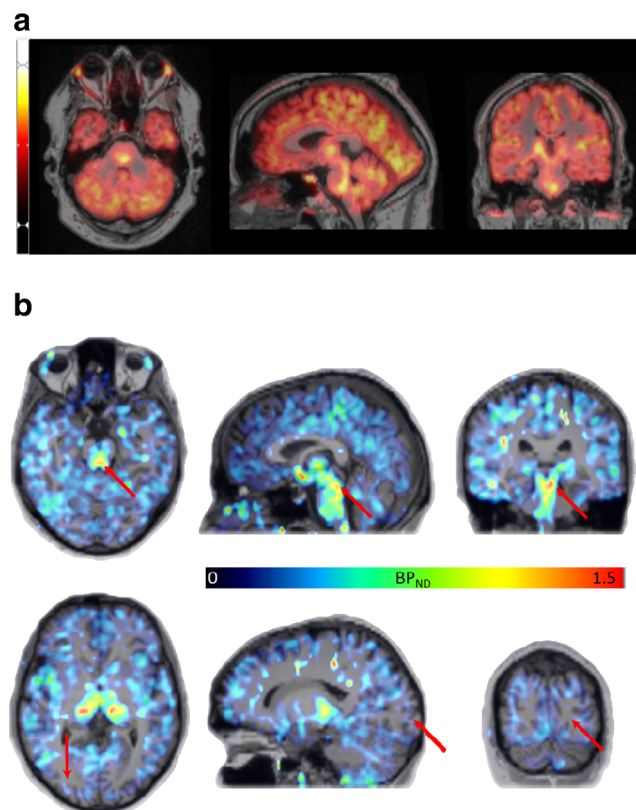


Fig. 1 Summed PET images (all frames of dynamic studies) (a) and BP_{ND} images (b) of $[^{11}\text{C}]\text{MRB}$ imaging data coregistered to the corresponding MRI T1 image. The arrow depicts the noradrenaline transporter-rich area of the locus coeruleus (middle row) and the occipital cortex as a reference region (lower row) in the BP_{ND} maps

There was significantly higher BP_{ND} in the left putamen in obese vs. non-obese individuals ($p = 0.028$). Significance was further increased ($p < 0.001$) when comparing hemispheric differences (Fig. 4). LDA with stepwise inclusion of variables identified five brain regions as most relevant in the discrimination of the two groups including the left putamen (most important), right putamen, raphe nuclei, pons/midbrain, and the LC (model 1; Table 4). The demographic variables age and sex were not included in the model in the selection process by the LDA, i.e. there were not significant. These two variables also showed no significant group difference in an unpaired *t* test. Reclassification performance using cross-validation (leave-one-out technique) of this 5-variable discriminant model was very high (Table 4) with 10 of 10 obese and 9 of 10 non-obese correctly classified (Wilk's lambda = 0.108; $p < 0.00001$). Based on these results, three more discriminant models were constructed and optimal separation was achieved using the left and right putamen, and the LC (Table 4).

We compared the occipital cortex and the caudate as reference regions. Mean BP_{ND} values were in good agreement, e.g. for non-obese subjects in the thalamus 0.41 ± 0.18 vs. 0.39 ± 0.20 , the LC 0.32 ± 0.20 vs. 0.33 ± 0.27 , as well as in the hypothalamus 0.46 ± 0.15 vs. 0.46 ± 0.25 (Table 2). Also, only in one brain region, the left putamen, there was a significantly different (higher) BP_{ND} in obese vs. non-obese individuals ($p = 0.016$) if the caudate was used as a reference region.

Discussion

The brain LC-NA system, in particular, its presynaptically located regulatory proteins for NA reuptake, the NATs, are thought to be involved in weight control and contribute to the pathogenesis of human obesity [21, 22]. However, only one study thus far has addressed the question of whether in vivo NAT availability is altered in obesity [9]. By applying

Table 2 Noradrenaline transporter binding potentials (BP_{ND})

Region	Obese subjects (<i>n</i> = 10)	Non-obese controls (<i>n</i> = 10)	<i>p</i> value
Medial prefrontal cortex	0.05 (0.09)	0.08 (0.06)	0.45
Orbito-frontal cortex	0.06 (0.12)	0.08 (0.14)	0.79
Dorsolateral prefrontal cortex	0.08 (0.09)	0.08 (0.06)	0.99
Anterior cingulate cortex	0.12 (0.12)	0.13 (0.07)	0.88
Insula	0.18 (0.10)	0.20 (0.08)	0.65
Hippocampus	0.01 (0.10)	0.03 (0.06)	0.63
Amygdala	0.04 (0.13)	0.07 (0.09)	0.61
Nucleus accumbens	0.11 (0.12)	0.13 (0.10)	0.73
Head of the caudate	0.02 (0.07)	0.03 (0.10)	0.67
Putamen	0.12 (0.12)	0.07 (0.08)	0.27
Thalamus	0.40 (0.14)	0.41 (0.18)	0.84
Pons/midbrain	0.01 (0.11)	0.06 (0.10)	0.17
Locus coeruleus	0.38 (0.22)	0.32 (0.20)	0.72
Hypothalamus	0.41 (0.18)	0.46 (0.15)	0.52

Data were given in mean (standard deviation; Note that for the one subject that did not obtain an MRI scan, the regions of interest were drawn from an averaged normal MRI scan.).

PET imaging with [¹¹C]MRB they found decreased thalamic NAT availability in a sample of 17 moderately obese individuals with a BMI of 34.7 ± 2.6 kg/m² compared to 17 lean individuals with a BMI of 23.1 ± 1.4 kg/m², all of whom were free of major medical illnesses including past or present neurological and Axis-I psychiatric disorder. The aim of our study was to replicate this initial finding with a second independent European cohort of highly selected, highly obese individuals with a BMI larger than 35 kg/m² compared to carefully matched, non-obese controls. The study criteria here comprised an exclusion of depressive (and other mental) disorder as well as physical conditions including metabolic diseases.

On a group level, we did not find any significant differences in NAT availability. This might be due to technical reasons (i.e. the different scanners used in each study), that is

high-resolution research tomography (HRRT) vs. ECAT EXACT HR+ or different radioactivities [(596 MBq [6]) and low (359 MBq, this investigation)] of [¹¹C]MRB administered. Thus, time-activity curves were marginally less noisy from injections of high radioactivity compared to those with low radioactivity; however, the outcome measures with high radioactivity were not evidently improved in a study in rhesus monkeys (albeit both amounts of radioactivity were high translated into humans) [23]. Nonetheless, the groups were well-matched on important characteristics, including sex, age, and injected mass with slightly but not significantly higher BDI values in the obese. Since findings of the previous NAT study were obtained in male participants alone [9], we additionally checked whether there were differences in NAT availability between obese and non-obese men and women in

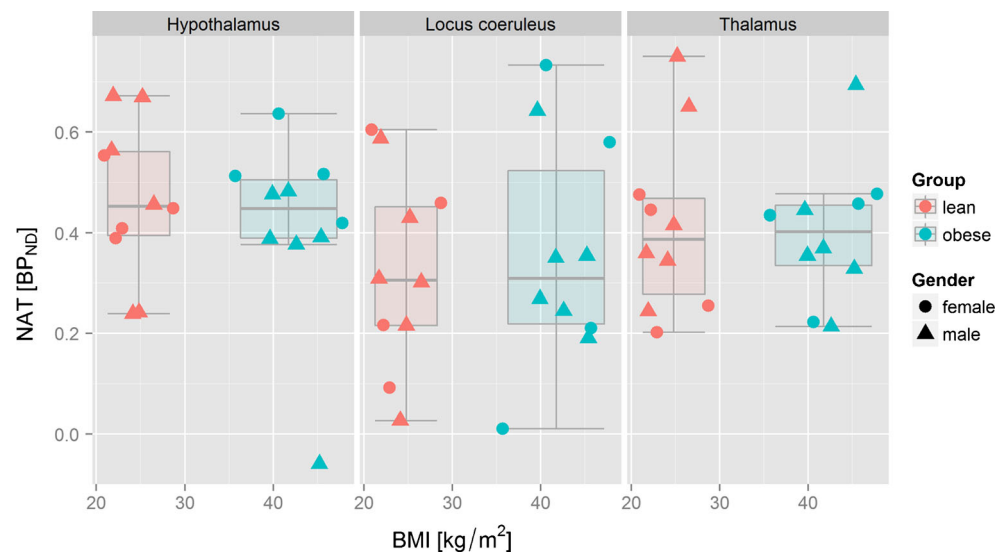
Fig. 2 Individual binding potential BP_{ND} values for correlation coefficients *r* and *p* values (see Tables 2 and 3)

Table 3 Coefficients of correlation between noradrenaline transporter binding potentials (BP_{ND}) and age/Beck Depression Inventory (BDI), and *p* values of group comparisons of BP_{ND} between obese and non-obese individuals after correction for age or BDI

Region	<i>r</i> : correlation with age	<i>r</i> : correlation with BDI	<i>p</i> (corrected for age)	<i>p</i> (corrected for BDI)
Medial prefrontal cortex	-0.20	-0.26	0.48	0.66
Orbito-frontal cortex	-0.15	-0.28	0.82	0.92
Dorsolateral prefrontal cortex	-0.25	-0.25	0.94	0.72
Anterior cingulate cortex	-0.42	-0.02	0.97	0.90
Insula	-0.36	-0.29	0.70	0.93
Hippocampus	-0.13	-0.38	0.66	0.99
Amygdala	0.07	-0.13	0.60	0.72
Nucleus accumbens	-0.07	-0.46*	0.62	0.94
Head of the caudate	0.33	-0.21	0.72	0.99
Putamen	0.36	-0.14	0.29	0.18
Thalamus	-0.04	0.10	0.85	0.74
Pons/midbrain	-0.19	-0.41	0.19	0.36
Locus coeruleus	-0.08	-0.22	0.71	0.50
Hypothalamus	-0.42	-0.06	0.56	0.56

**p* < 0.05

our sample of only four females and six males each. We found very small differences (*t* test) between obese and non-obese in males for the (left) prefrontal cortex (*p* = 0.022 vs. *p* = 0.38 in women); and for females in the (left) cerebellar cortex (*p* = 0.017; male: *p* = 0.21); however, we were not able to reproduce a clear finding in males alone.

[¹¹C]MRB is currently the most promising radiotracer for imaging NAT availability. However, as pointed out previously, its use has limitations [9]. These include low binding potential, which could artificially introduce between-group differences if between-group differences arise at the level of non-displaceable binding, in particular in cortical areas or in the striatum, that are all areas with low NAT densities in the central nervous system (CNS). Additionally, the magnitudes of

changes in modulatory systems, to which the NA fibres belong, are also relatively low and, so, noise reduction is often achieved at the expense of accuracy. Consequently, there is an inherent limitation concerning the reproducibility of this technique: Combined with the relatively low resolution of the applied scanner and the poor signal-to-noise ratio of the administered NAT ligand, thus the interpretability in relevant NA areas with relatively low NAT expression such as cortical regions, the hippocampus, and the striatum shall be carefully considered. Both studies used the occipital cortex as a region low in NAT and, thus, for an estimate of non-displaceable

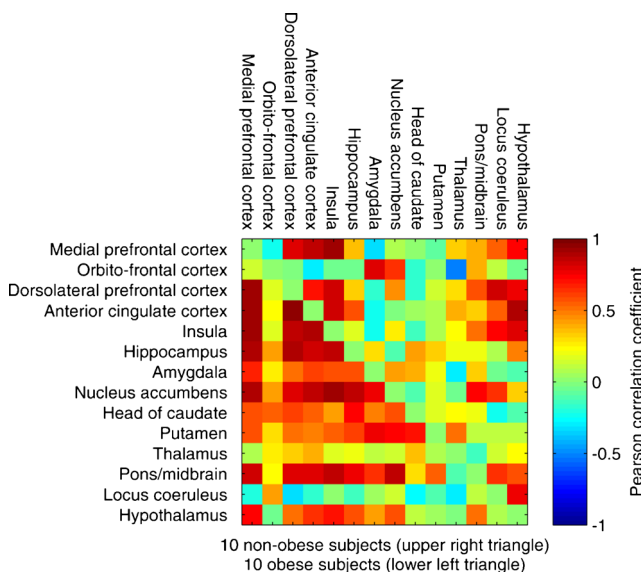


Fig. 3 Correlation matrix of inter-regional BP_{ND} associations

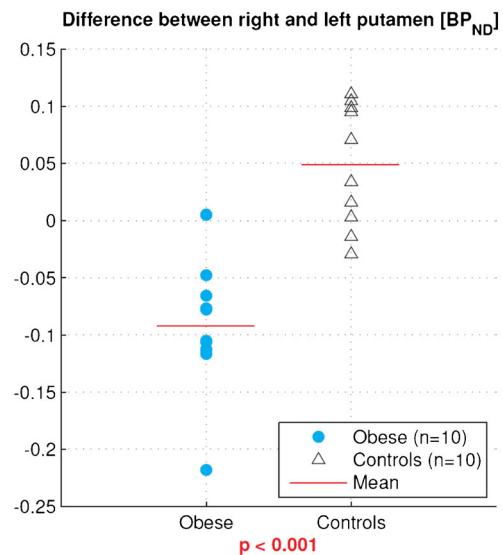


Fig. 4 Difference of binding potential BP_{ND} values between the right and left putamen: Obese and non-obese individuals showed highly significant differences of asymmetry between the right and the left putamen. This explains the high discrimination power of only two variables (putamen left and putamen right) in the discriminant analysis

Table 4 Linear discriminant analysis based on five brain regions (Model 1)

Results of classification	Group	Predicted		Total
		Non-obese	Obese	
		Reclassification of original cases (number/%)	Non-obese	
	Obese	0/0.0	10/100.0	10/100.0
Reclassification by cross-validation ^a (number/%)	Non-obese	9/90.0	1/10.0	10/100.0
	Obese	0/0.0	10/100.0	10/100.0

a. Cross-validation was performed only for cases of this analysis. Herein, every case was classified by a function which was derived from all other cases except the present one (leave-one-out technique)

Alternative models

Model 2 (left, right putamen, locus coeruleus)

Reclassification performance: 10 of 10 OB and 9 of 10 HCs were correctly classified yielding a sensitivity of 100% and specificity of 90% (Wilk's lambda = 0.261, $p < 0.0001$). Same reclassification results by cross-validation as in model 1. Correct reclassification rate of 95%

Model 3 (left, right putamen, pons/midbrain)

Reclassification performance using cross-validation: 8 of 10 obese subjects (OB) and 10 of 10 healthy controls (HCs) were correctly classified yielding a sensitivity of 80% and specificity of 100% (Wilk's lambda = 0.258, $p < 0.0001$). Correct reclassification rate of 90%

Model 4 (left, right putamen)

Reclassification performance: 9 of 10 OB and 8 of 10 HCs were correctly classified yielding a sensitivity of 90% and specificity of 80% (Wilk's lambda = 0.356, $p < 0.001$). Correct reclassification rate of 85%

binding [17, 24]. The caudate region was likewise used as a reference region when quantifying the NAT in patients with attention deficit disorder using an ^{18}F -labelled compound [25]. In our analysis, the two reference regions, the occipital cortex and caudate, showed very similar BP_{ND} group means and both identified equally only the left putamen as showing a significant difference in obese and non-obese individuals' transporter status. So, both brain regions can and are used as reference regions for the quantification of NAT availability but the much larger volume of the occipital cortex is favourable.

As in the study by Li et al. [9], we obtained here regionally specific effects, which could in part be ascribed to a between-group difference in non-displaceable binding. This might be the case for the (left) putamen, a region that is regularly found to be involved in the regulation of eating behaviour [13]. The discriminant analysis revealed that it is BP_{ND} in the left and right putamen that correctly classifies 9 of 10 obese and 8 of 10 non-obese subjects (Table 4). This surprising result finds its explanation in the observation that it is the BP_{ND} difference between the right and left putamen that is substantially different (Fig. 4). If it is indeed a right/left hemispheric NAT difference in the putamen that distinguishes obese and non-obese humans, this requires further investigations. Furthermore, LDA based on the NAT-rich LC revealed a relatively high power to distinguish obese from non-obese humans. Together with this, correlative analyses point towards a distinctive regional distribution of NAT availability between

obese and non-obese individuals with more robust associations in obese individuals as we have found also for serotonin transporters [26]. This observational finding should be discussed with other parameters of neural connectivity in the near future to obtain specific group characteristics. Further work on our sample in parallel with these data included associative analyses with resting-state functional MRI data and neuropsychological measures showing initial findings of NAT-based interaction of neuronal and behavioural activity [27]. Within this further data processing we showed that an increased BMI is related to a lowered NAT availability in the hypothalamus together with changes in a network mediating emotional well-being. We did not, however, observe a significant between-group difference in NAT availability in the hypothalamus. This is of interest, since the hypothalamus is the metabolic centre and has been implicated in NA dysfunction in association with obesity. Nevertheless, the initial study by Li et al. also failed to identify NAT changes in the hypothalamus in obesity [9].

In the present study, there were strict restrictions on eating or fasting periods although study participants were encouraged to have a light breakfast on the day prior to PET scanning. This is in accordance with other PET studies investigating monoamine transporters in cases of obesity [28]. Although the immediate effects on NA release or NA-associated network changes associated with feeding state prior to scanning cannot be excluded, we assume measuring transporters are

insensitive to short-term fluctuations in neurotransmitter levels, as has been shown for the serotonin transporter [29].

One further limitation of the current study is, although adequate for a PET study, the sample size is relatively small. Future studies employing a larger sample size might reveal important individual differences or the influence of gender, stress and genotypes that have been linked to important aspects of eating behaviours and obesity. This is particularly important in light of recent studies on the brain monoaminergic transporter system that also did not show an association between BMI and transporter binding potential across the entire sample [27, 30].

Conclusions

Although we failed to replicate the initial findings of decreased NAT availability in the NET-rich thalamus in obesity, the NAT availability in other NAT-rich regions such as the hypothalamus and the LC was similar between obese and non-obese study participants consistent with the previous study. Furthermore, preliminary secondary findings of distinct regional and associative patterns of our study on NAT in highly obese, non-depressed individuals warrant further investigation, including larger groups of obese individuals with specific patterns of eating behaviour (e.g., an over-eating phenotype), endocrine and neural parameters. Such data will help to overcome the lack of a biological footing across a range of neuropsychological disorders including obesity with implications for their future diagnostic, therapeutic and preventive strategies.

Acknowledgements The work is supported by the IFB Adiposity Diseases, Federal Ministry of Education and Research (BMBF), Germany, FKZ: 01E01001 (<http://www.bmbf.de>). Results of the study were partially presented at the 29th World Congress of The International College of Neuropsychopharmacology, 2014, in Vancouver, Canada, and at the 26th Annual Congress of the European Association of Nuclear Medicine, 2013, Lyon, France.

Compliance with ethical standards

Funding This study was supported by the German Federal Ministry of Education and Research (FKZ: 01E01001).

Conflict of interest The authors declare no conflicts of interest directly related to the subject of this work.

Ethical approval All procedures performed in studies involving human participants were in accordance with the ICH Guideline for Good Clinical Practice (GCP) and with the 1964 Helsinki Declaration and its later amendments. The study was approved by the ethics committee of the Medical Faculty of the University of Leipzig (registered under the number 206-10-08032010) and the German Bundesamt für Strahlenschutz/Federal Office for Radiation Protection (number Z5-22461-2-2011-002), and registered at the European Clinical Trial Database (EudraCT 2012-000568-32) and the German Clinical Trials Register (DRKS).

Informed consent Informed consent was obtained from all individual participants included in the study.

References

- Nelson DL, Gehlert DR. Central nervous system biogenic amine targets for control of appetite and energy expenditure. *Endocrine*. 2006;29:49–60.
- Adan RA, Vanderschuren LJ, la Fleur SE. Anti-obesity drugs and neural circuits of feeding. *Trends Pharmacol Sci*. 2008;29:208–17.
- Leibowitz SF. Reciprocal hunger-regulating circuits involving alpha- and beta-adrenergic receptors located, respectively, in the ventromedial and lateral hypothalamus. *Proc Natl Acad Sci U S A*. 1970;67:1063–70.
- Alexander JT, Cheung WK, Dietz CB, Leibowitz SF. Meal patterns and macronutrient intake after peripheral and PVN injections of the alpha 2-receptor antagonist idazoxan. *Physiol Behav*. 1993;53:623–30.
- Date Y, Shimbara T, Koda S, Toshinai K, Ida T, Murakami N, et al. Peripheral ghrelin transmits orexigenic signals through the noradrenergic pathway from the hindbrain to the hypothalamus. *Cell Metab*. 2006;4:323–31.
- Lee SJ, Diener K, Kaufman S, Krieger J, Pettersen KG, Jejelava N, et al. Limiting glucocorticoid secretion increases the anorexigenic property of Exendin-4. *Mol Metab*. 2016;5:552–65.
- Tovar S, Paeger L, Hess S, Morgan DA, Hausen AC, Brönneke HS, et al. K(ATP)-channel-dependent regulation of catecholaminergic neurons controls BAT sympathetic nerve activity and energy homeostasis. *Cell Metab*. 2013;18:445–55.
- Dallman MF. Stress-induced obesity and the emotional nervous system. *Trends Endocrinol Metab*. 2010;21:159–65.
- Li CS, Potenza MN, Lee DE, Planeta B, Gallezot JD, Labaree D, et al. Decreased norepinephrine transporter availability in obesity: Positron Emission Tomography imaging with (S, S)-[¹¹C]O-methylreboxetine. *Neuroimage*. 2015;86:306–10.
- Schulz P, Macher JP. The clinical pharmacology of depressive states. *Dialogues Clin Neurosci*. 2002; 47–56.
- Hautzinger M. The beck depression inventory in clinical practice. *Nervenarzt*. 1991;62:689–96.
- Hilbert A, Tuschen-Caffier B. Eating disorder examination: Deutschsprachige Übersetzung. Münster: Verlag für Psychotherapie; 2006.
- Lin KS, Ding YS. Synthesis, enantiomeric resolution, and selective C-11 methylation of a highly selective radioligand for imaging the norepinephrine transporter with positron emission tomography. *Chirality*. 2004;16:475–81.
- Hesse S, Brust P, Mäding P, Becker GA, Patt M, Seese A, et al. Imaging of the brain serotonin transporters (SERT) with ¹⁸F-labelled fluoromethyl-McN5652 and PET in humans. *Eur J Nucl Med Mol Imaging*. 2012;39:1001–11.
- Horstmann A, Busse FP, Mathar D, Müller K, Lepsien J, Schlögl H, et al. Obesity-related differences between women and men in brain structure and goal-directed behavior. *Front Hum Neurosci*. 2011;5: 58.
- Bertoldo A, Cobelli C. Physiological modelling of positron emission tomography images. In: Carson E, Cobelli C, editors. *Modelling methodology for physiology and medicine*. London: Elsevier; 2014. p. 417–48.
- Ichise M, Liow JS, Lu JQ, Takano A, Model K, Toyama H, et al. Linearized reference tissue parametric imaging methods: application to [¹¹C]DASB positron emission tomography studies of the

- serotonin transporter in human brain. *J Cereb Blood Flow Metab.* 2003;9:1096–112.
18. Pietrzak RH, Gallezot JD, Ding YS, Henry S, Potenza MN, Southwick SM, et al. Association of posttraumatic stress disorder with reduced in vivo norepinephrine transporter availability in the locus coeruleus. *JAMA Psychiat.* 2013;70:1199–205.
 19. Innis RB, Cunningham VJ, Delforge J, Fujita M, Gjedde A, Gunn RN, et al. Consensus nomenclature for in vivo imaging of reversibly binding radioligands. *J Cereb Blood Flow Metab.* 2007;27:1533–9.
 20. Becker GA, Ichise M, Barthel H, Luthardt J, Patt M, Seese A, et al. PET quantification of ^{18}F -florbetaben binding to β -amyloid deposits in human brains. *J Nucl Med.* 2013;54:723–31.
 21. Guimarães J, Moura E, Silva E, Aguiar P, Garrett C, Vieira-Coelho MA. Locus coeruleus is involved in weight loss in a rat model of Parkinson's disease: an effect reversed by deep brain stimulation. *Brain Stimul.* 2013;6:845–55.
 22. Hainer V, Kabmova K, Aldhoon B, Kunesova M, Wagenknecht M. Serotonin and norepinephrine reuptake inhibition and eating behavior. *Ann N Y Acad Sci.* 2006;1083:252–69.
 23. Takano A, Gulyás B, Varrone A, Halldin C. Comparative evaluations of norepinephrine transporter radioligands with reference tissue models in rhesus monkeys: (S, S)- ^{18}F FMENR-D2 and (S, S)- ^{11}C MeNER. *Eur J Nucl Med Mol Imaging.* 2009;36:1885–91.
 24. Hannestad J, Gallezot JD, Planeta-Wilson B, Lin SF, Williams WA, van Dyck CH, et al. Clinically relevant doses of methylphenidate significantly occupy norepinephrine transporters in humans in vivo. *Biol Psychiatry.* 2010;68:854–60.
 25. Vanicek T, Spies M, Rami-Mark C, Savli M, Höflich A, Kranz GS, et al. The norepinephrine transporter in attention-deficit/hyperactivity disorder investigated with positron emission tomography. *JAMA Psychiat.* 2014;71:1340–9.
 26. Hesse S, Rullmann M, Luthardt J, Winter K, Hankir MK, Becker GA, et al. Central serotonin transporter availability in highly obese individuals compared with non-obese controls: A ^{11}C DASB positron emission tomography study. *Eur J Nucl Med Mol Imaging.* 2016;43:1096–104.
 27. Melasch J, Rullmann M, Hilbert A, Luthardt J, Becker GA, Patt M, et al. The central nervous norepinephrine network links a diminished sense of emotional well-being to an increased body weight. *Int J Obes.* 2016;40:779–87.
 28. Haahr ME, Hansen DL, Fisher PM, Svarer C, Stenbæk DS, Madsen K, et al. Central 5-HT neurotransmission modulates weight loss following gastric bypass surgery in obese individuals. *J Neurosci.* 2015;35:5884–9.
 29. Paterson LM, Tyacke RJ, Nutt DJ, Knudsen GM. Measuring endogenous 5-HT release by emission tomography: promises and pitfalls. *J Cereb Blood Flow Metab.* 2010;30:1682–706.
 30. van de Giessen E, Hesse S, Caan MW, Zientek F, Dickson JC, Tossici-Bolt L, et al. No association between striatal dopamine transporter binding and body mass index: a multi-center European study in healthy volunteers. *Neuroimage.* 2013;64:61–7.